

Design of reconfigurable frequency-selective surfaces including the PIN diode threshold region

 ISSN 1751-8725
 Received on 11th August 2017
 Revised 25th February 2018
 Accepted on 1st March 2018
 E-First on 9th April 2018
 doi: 10.1049/iet-map.2017.0761
 www.ietdl.org

 Deisy Formiga Mamedes^{1,2}, Alfrêdo Gomes Neto^{1,2} ✉, Jefferson Costa e Silva^{1,2}, Jens Bornemann³
¹Federal Institute of Paraíba, João Pessoa, Paraíba, Brazil

²Group of Telecommunication and Applied Electromagnetism – GTEMA-IFPB, João Pessoa, Paraíba, Brazil

³Department of Electrical and Computer Engineering, University of Victoria, Victoria, BC, V8W 2Y2, Canada

✉ E-mail: alfredogomes@ifpb.edu.br

Abstract: Reconfigurable frequency-selective surfaces (RFSSs) are of significant interest in applications, such as secure communication systems or tunable radomes, to improve indoor communication and smart antennas. In order to change the frequency-selective surface (FSS) characteristics, and therefore its frequency response, conventional methods include loading with active semiconductor devices such as varactors, PIN diodes, Schottky diodes and radio-frequency microelectromechanical system. Another possibility is the use of mechanical adjusts, such as spring resonators or mechanical rotation. When PIN diodes are used, commonly only the reverse and forward regions, OFF and ON states, respectively, are considered. In this study, the implementation of an RFSS is described, using PIN diodes as active components. The RFSS is based on the four-arms star geometry, and initial design equations and procedures are presented. Numerical and measured results are shown for different project stages, with a very good agreement. In addition to obtaining two distinct resonant frequencies, due to the OFF and ON states, a third situation is included, considering the PIN diode threshold region when the FSS becomes practically transparent, which is an interesting feature with potential applications.

1 Introduction

Frequency-selective surfaces (FSSs) have been widely investigated in recent years, both in passive (FSS) and reconfigurable FSS (RFSS) variations. Intelligent walls [1–4], radomes [5, 6], and reconfigurable antennas [7–9] are some examples of their applications. Essentially, an FSS consists of basic elements etched on a dielectric substrate, arranged in a planar periodic structure, providing filtering properties. The FSS frequency response depends on the polarisation of the incident wave, the geometry of the planar circuit and the spacing between the elements within the FSS structure, and the substrate thickness and permittivity [10] (Fig. 1). The planar FSS type is also referred as 2D FSS, in contrast to the 3D FSS whose basic elements are 3D [11, 12].

In order to achieve RFSS characteristics, two main approaches are considered: mechanical tuning and insertion of discrete electronic components. Mechanically tunable FSSs can be implemented by exploiting mechanical modifications such as stretching, folding, shifting or rotating the FSS elements [11–13]. Insertion of discrete electronic components includes PIN diodes [7–9], microelectromechanical (MEMS) switches [14, 15], and

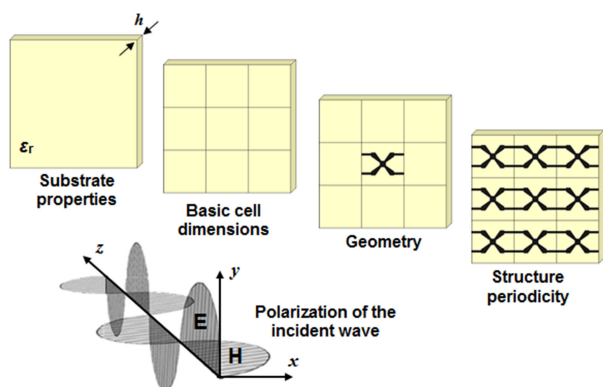


Fig. 1 FSS geometry and parameters that affect the FSS frequency response

varactors [16, 17]. When PIN diodes are used, commonly only the reverse and the forward regions, OFF and ON states, respectively, are taken into account.

In this paper, the PIN diode threshold region is included and in addition to obtaining two distinct resonant frequencies, due to the OFF and the ON states, a third situation is now obtained where the FSS becomes practically transparent, which is a very interesting feature. In addition to the material presented in [18], this paper presents initial design guidelines, investigates the influence of bias lines and adds PIN diodes for truly RFSSs.

2 RFSS design and implementation

One of the most adjustable parameters in the design of the FSS is the geometry of the unit cell. In this paper, the RFSS is based on the four-arms star geometry (Fig. 2). This geometry was introduced in [18, 19] with very interesting characteristics such as miniaturisation and switch applications. For an ideal switch, the OFF state is represented by a gap and the ON state by a metallic strip, as shown in Figs. 2a and b, respectively. The gap width is defined by the PIN diode dimensions.

In order to obtain this geometry, an FSS with conventional rectangular patch elements is initially designed, and the basic cell dimensions W_x , W_y , L_x and L_y are determined (Fig. 3a). In addition to this rectangular patch, a switch point is introduced as shown in Figs. 3b and c. From the edges, lines cross the rectangular patch

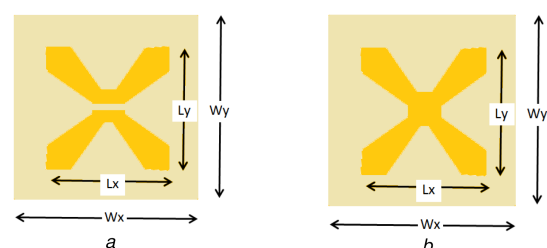


Fig. 2 Four-arms star geometry (a) Ideal OFF state, (b) Ideal ON state

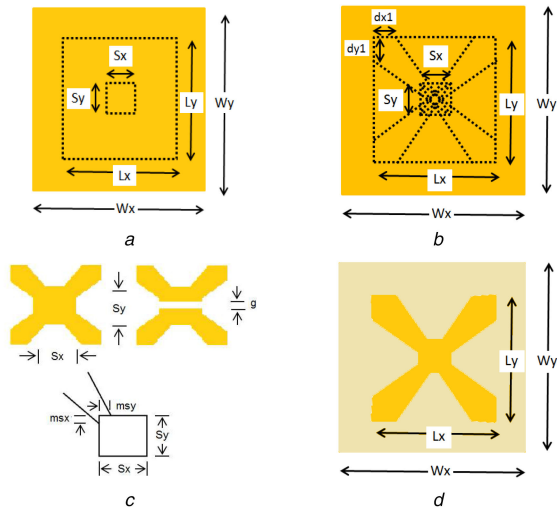


Fig. 3 Four-arms star geometry step-by-step
(a) Basic cell with rectangular patch and switch point, (b) Lines cross the rectangle from the edges, (c) Switch point details, (d) Four-arms star geometry



Fig. 4 Four-arms star geometry with PIN diode
(a) PIN diode inserted, (b) Bias lines added

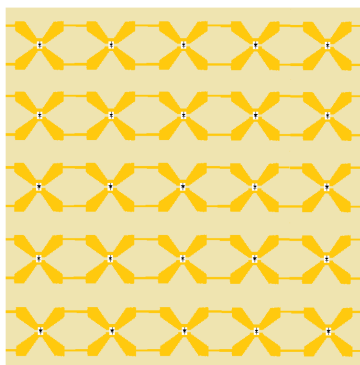


Fig. 5 Example of a 5×5 RFSS

(Fig. 3b), and the four-arms star geometry is achieved. Finally, the outside parts of the four arms are detached from the metallic surface, and the four-arms star is completed (Fig. 3d).

The four-arms star geometry is polarisation dependent. Considering ideal states, if the electric field is horizontally polarised (x -direction), OFF and ON states do not affect the frequency response. However, if the electric field is vertically polarised (y -direction), the OFF state resonant frequency will be approximately twice that of the ON state [18, 19]. This is due to the fact that in the OFF state, the geometry is composed of two separate parts (Fig. 2a) but in the ON state (Fig. 2b), the two parts are joined, and the effective length is approximately doubled.

Determining the dimensions of the FSS basic cell element is a process often based on the designer's experience and usually an iterative procedure. After establishing an initial value, the design is optimised until the desired characteristics are achieved. Therefore, an expression to estimate the first resonant frequency of the FSS will help in the design procedure, and (1) [20] provides good results if the substrate thickness $h \ll \lambda_0$

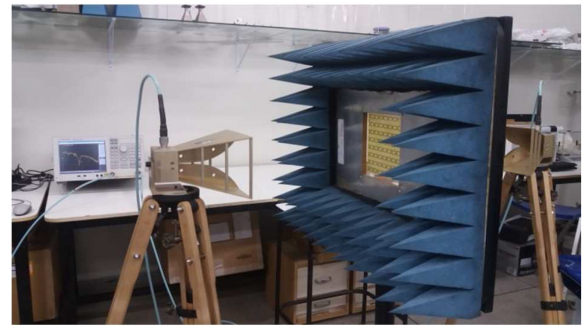


Fig. 6 Measurement setup

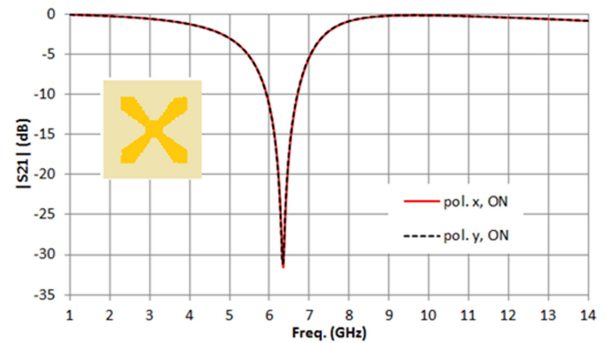


Fig. 7 Four-arms star frequency response, ON state

$$f_{\text{res}}(\text{GHz}) = \frac{0.3}{2l_{\text{efe}}} \quad (1)$$

where $l_{\text{efe}} = Lx + Ly$.

Note that in (1), the effective relative permittivity is ignored due to the fact that the substrate thickness is much smaller than the wavelength, thus resulting in $\epsilon_{\text{reff}} \approx 1$. It is also worth mentioning that (1) is only an initial equation, i.e. the first step towards a numerical optimisation process.

The PIN diode is inserted into the switch point, as depicted in Fig. 4a. The next step is to add bias lines (Fig. 4b). Then the basic cell is reproduced as shown for a 5×5 example in Fig. 5. Note that each line can be biased separately, which is an interesting feature, whether to test the diodes during the RFSS manufacturing process or to obtain different reconfiguration arrangements.

3 Results and discussions

Numerical results were obtained using the commercial software package ANSYS HFSS 15.0. The measured results were obtained at the GTEMA/IFPB microwave measurements laboratory using an Agilent E5071C two-port network analyser, two double ridge horn antennas and a measurement window as shown in Fig. 6. The wave incidence is considered normal to the RFSS.

As a first step, two FSSs based on the four-arms star geometry, without the bias lines, were designed and numerically characterised. The first one corresponds to the ON state (Fig. 7) and the second one to the OFF state (Fig. 8). A low cost dielectric substrate FR-4 ($\epsilon_r = 4.4$, height $h = 1.0$ mm, and loss tangent of 0.02) was used. The four-arms star geometry dimensions are (cf. Fig. 3): $Wx = Wy = 22.5$ mm, $Lx = Ly = 12.0$ mm, $dx = dy = 2.0$ mm, $Sx = Sy = 3.0$ mm, $msx = msy = 0.75$ mm, and the gap, when present, $g = 1.0$ mm. As expected, for the ON state, the geometry is symmetric, and for both polarisations, the frequency response is identical (Fig. 7). When compared to the resonant frequency of 6.25 GHz as obtained from (1), the numerical result of 6.35 GHz presents a good agreement.

Fig. 8 shows that for the OFF state, the x polarisation frequency response remains practically the same as that of the ON state. However, the y polarisation resonant frequency is 11.47 GHz, corresponding to a ratio $f_{\text{rOFF}}/f_{\text{rON}} \approx 1.81$, which is a feature adequate for RFSS needs. Please note that the frequencies of 6.25

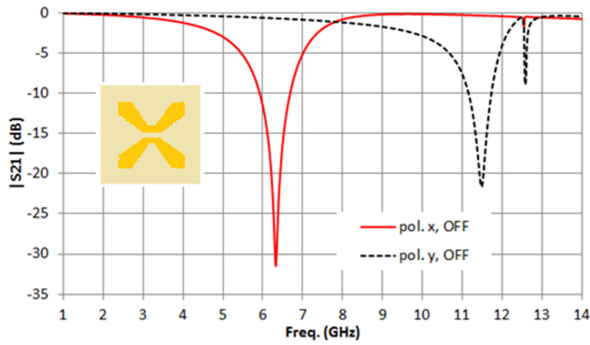


Fig. 8 Four-arms star frequency response, OFF state

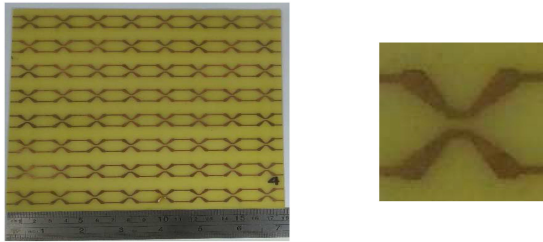


Fig. 9 Fabricated RFSS and individual cell without PIN diodes, ideal OFF state

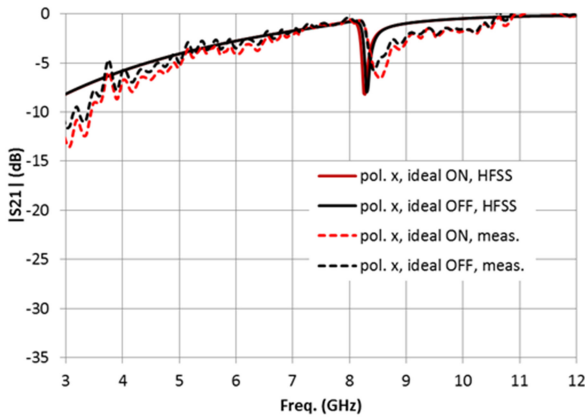


Fig. 10 Simulated and measured FSS ideal ON and OFF states, polarisation x

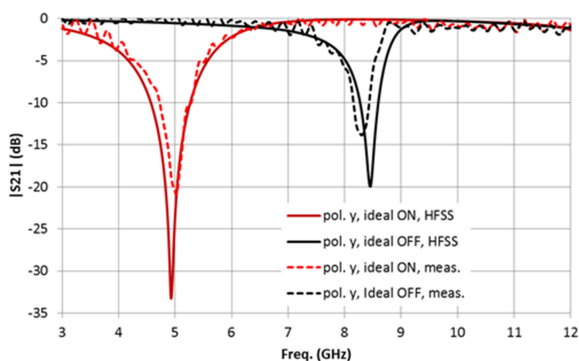


Fig. 11 FSS ideal ON and OFF states, polarisation y

and 11.47 GHz were selected to fall within the range of our measurement setup.

The next step is to add the bias lines, using a width of 1.0 mm, and to insert the PIN diodes, as depicted in Figs. 4 and 5. The selected PIN diode is the BAR 64-03 W (Infineon Technologies) with the following characteristics:

- forward current: 100 mA,
- reverse voltage: 150 V,
- forward voltage: 1.1 V, at $I_F = 50$ mA,

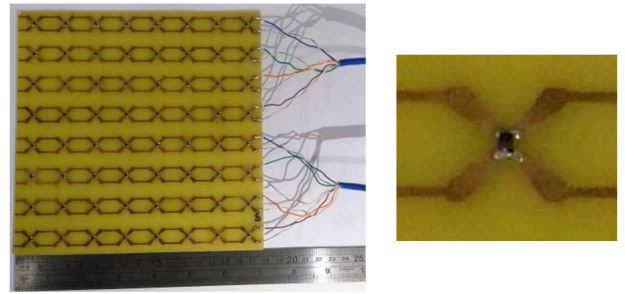


Fig. 12 Fabricated RFSS and unit cell with bias lines and PIN diodes

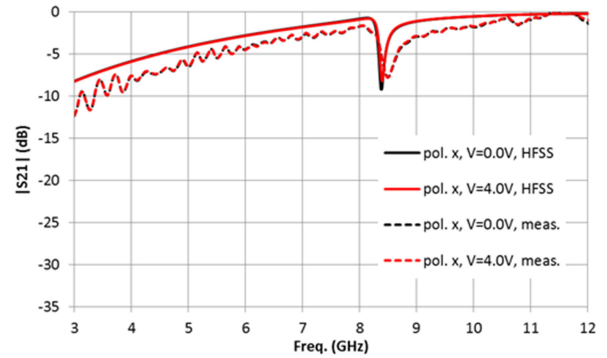


Fig. 13 Simulated and measured RFSS ON and OFF states, polarisation x

- forward resistance: 2.8Ω (max.) at $I_F = 10$ mA,
- capacitance: 0.35 pF (max.),
- frequency range above 1 MHz up to 6 GHz.

Three RFSSs were fabricated, with 8×8 unit cells, corresponding to total dimensions of $180 \text{ mm} \times 180 \text{ mm}$. Two of them do not include the PIN diode; they are the ideal OFF state (Fig. 9) and the ON state. However, they include the bias lines in order to evaluate the influence of the bias lines on the frequency response. The third prototype includes the PIN diodes and allows evaluation of the RFSS's behaviour as well as the inclusion of the PIN diode threshold.

In Fig. 10, numerical and measured results are shown in horizontal (x) polarisation, with a very good agreement. As expected, ON and OFF states present practically the same frequency response. Note that compared to Fig. 7, the resonant frequency is shifted upwards as a result of adding the bias lines.

For vertical (y) polarisation, numerical and measured results are compared in Fig. 11, and very good agreement is observed. Note that for the ideal ON state, the resonant frequency is 5.05 GHz, corresponding to a ratio $f_{r\text{OFF}}/f_{r\text{ON}} \approx 1.66$, not so different from the four-arm star without the bias lines. However, with the bias lines, the resonant frequencies are $\sim 75\%$ of the values for the four-arm star without bias lines (Fig. 8). This is an expected result since the presence of the bias lines increases the inductive and capacitive effects. We have to highlight here that the resonant frequency reduction depends on the number of basic cells, but it can be numerically optimised.

The third prototype, the RFSS with bias lines and PIN diodes, is shown in Fig. 12. A 150Ω resistor limits the PIN diode currents for each line. For horizontal (x) polarisation, numerical and measured results are presented in Fig. 13 for OFF (0.0 V) and ON (4.0 V) states, with the very good agreement. The results are similar to those of the ideal OFF and ON states in Fig. 10.

For vertical (y) polarisation, numerical and measured results are presented in Fig. 14. Despite minor differences observed for the ON state (4.12 GHz), a good agreement is verified. The ratio $f_{r\text{OFF}}/f_{r\text{ON}} = 6.72 \text{ GHz}/4.12 \text{ GHz} \approx 1.63$ remains practically the same when compared to that of the ideal states with bias lines, but resonant frequencies are reduced to $\sim 80\%$. The parasitic effects due to the insertion of the PIN diodes justify this frequency reduction. Roughly, we can consider that the proposed RFSS including bias lines and PIN diodes has resonant frequencies that

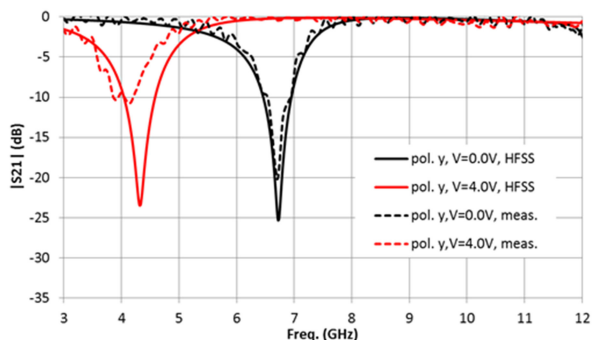


Fig. 14 Simulated and measured RFSS ON and OFF states, polarisation y

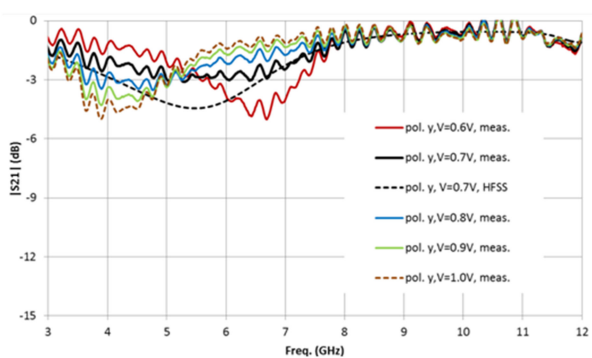


Fig. 15 Simulated and measured RFSS, polarisation y , PIN diodes threshold region

are 60% smaller than observed from the four-arm star in Figs. 7 and 8.

Although the OFF and ON states are usually highlighted in RFSS applications, another region can be exploited. When the PIN diodes are near their threshold region, a very interesting result is observed. Switching from the OFF state to the ON state, the PIN diodes change the geometry's effective length and its respective resonance; it behaves like a band-stop filter. However, in the threshold region, the RFSS is practically an all-pass filter, as it can be seen in Fig. 15. Wide-band applications, such as smart antennas for UWB, can profit from this feature to obtain a configuration where no frequency band is rejected, in addition to the choice between the two reject bands. To the best of our knowledge, such region has not been explored in RFSS design and, unfortunately, we cannot affirm that this all-pass region will be present when using other geometries or bias configurations. The detailed investigation of this interesting research topic is beyond the scope of the paper.

4 Conclusion

The implementation of an RFSS is detailed, from the geometry of the basic four-arms star cell to the integration of bias lines and PIN diodes. Initial design equations are capable of establishing the geometry dimensions starting with the desired resonant frequency, and a ratio $f_{r\text{OFF}}/f_{r\text{ON}} = 6.72 \text{ GHz}/4.12 \text{ GHz} \simeq 1.63$ is achieved. Implementation stages present numerical and measured results and very good agreement is observed.

Different from other works, we not only considered the OFF and ON stages of the PIN diode but also described the effect of the PIN diode threshold region, where the RFSS becomes practically transparent. This is a very interesting feature with many potential applications.

5 References

- [1] Subrt, L., Pechac, P.: 'Intelligent walls as autonomous parts of smart indoor environments', *IET Commun.*, 2012, **6**, (8), pp. 1004–1010
- [2] Gustafsson, M., Karlsson, A., Pontes Rebelo, A.P., *et al.*: 'Design of frequency selective windows for improved indoor outdoor communication', *IEEE Trans. Antennas Propag.*, 2006, **54**, (6), pp. 1897–1900
- [3] Habib, S., Kiani, G.I., Butt, M.F.U.: 'Interference mitigation and WLAN efficiency in modern buildings using energy saving techniques and FSS'. IEEE AP-S Int. Symp. Digest (APS/URSI), Fajardo, Puerto Rico, July 2016, pp. 965–966
- [4] Ullah, I., Zhao, X., Habibih, D., *et al.*: 'Transmission improvement of UMTS and Wi-Fi signals through energy saving glass using FSS'. Proc. IEEE Wireless Microwave Technology Conf. (WAMICON), Clearwater, FL, USA, April 2011, pp. 1–5
- [5] Sangeetha, B., Gulati, G., Nair, R.U., *et al.*: 'Design of airborne radome using Swastika-shaped metamaterial-element based FSS'. Proc. IEEE Annual India Conf. (INDICON), Bangalore, India, December 2016, pp. 1–4
- [6] Weiwei, W., Xi, C., Qi, F., *et al.*: 'A measured FSS radome with two absorptive bands separated by one passband'. Proc. 11th European Conf. Antennas Propagation (EUCAP), Paris, France, 2017, pp. 1118–1121
- [7] Al-Hasan, M.J., Denidni, T.A., Sebak, A.R.: 'Millimeter-wave FSS-based dielectric resonator antenna with reconfigurable radiation pattern'. IEEE AP-S Int. Symp. Digest, (APS/URSI), Memphis, TN, USA, July 2014, pp. 1441–1442
- [8] Bouslama, M., Traii, M., Denidni, T.A., *et al.*: 'Reconfigurable frequency selective surface for beam-switching applications', *IET Microw. Antennas Propag.*, 2017, **11**, (1), pp. 69–74
- [9] Sanz-Izquierdo, B., Liang, B., Parker, E.A., *et al.*: 'An application of active frequency selective surface to reconfigurable antenna technology'. Proc. Active and Passive RF Devices Seminar, London, UK, February 2016, pp. 1–5
- [10] Munk, B.A.: 'Frequency selective surfaces – theory and design' (Wiley & Sons, New York, 2000)
- [11] Ferreira, D., Cuiñas, I., Caldeirinha, R.F.S., *et al.*: '3-D mechanically tunable square slot FSS', *IEEE Trans. Antennas Propag.*, 2017, **61**, (1), pp. 242–250
- [12] Azemi, S.N., Ghorbani, K., Rowe, W.S.T.: 'A reconfigurable FSS using a spring resonator element', *IEEE Antennas Wirel. Propag. Lett.*, 2013, **12**, pp. 781–784
- [13] Abadi, S.M.A.M.H., Booske, J.H., Behdad, N.: 'Exploiting mechanical flexure as a means of tuning the responses of large-scale periodic structures', *IEEE Trans. Antennas Propag.*, 2016, **64**, (3), pp. 933–943
- [14] Lu, Z., She, J., Yan, X.: 'A dual-band reconfigurable FSS composite structure based on MEMS switches'. Proc. 11th Int. Symp. Antennas Propagation EM Theory (ISAPE), Guilin, China, October 2016, pp. 630–632
- [15] Safari, M., Shafai, C., Shafai, L.: 'X-Band tunable frequency selective surface using MEMS capacitive loads', *IEEE Trans. Antennas Propag.*, 2015, **63**, (3), pp. 1014–1021
- [16] Roberts, J., Ford, K.L., Rigelsford, J.M.: 'Secure electromagnetic buildings using slow phase-switching frequency-selective surfaces', *IEEE Trans. Antennas Propag.*, 2016, **64**, (1), pp. 251–261
- [17] Ebrahimi, A., Shen, Z., Withayachumnankul, W., *et al.*: 'Varactor-tunable second-order bandpass frequency-selective surface with embedded bias network', *IEEE Trans. Antennas Propag.*, 2016, **64**, (5), pp. 1672–1680
- [18] Gomes Neto, A., de Carvalho, J.N., da Silva, A.N., *et al.*: 'Four arms star: an useful geometry for switchable FSS'. Proc. SBMO/IEEE MTT-S Int. Microwave and Optoelectronics Conf., Rio de Janeiro, Brazil, August 2013, pp. 1–5
- [19] Lima, I.S.S.: 'Characterization of FSS with four arms star geometry'. Master Dissertation, IFPB, João Pessoa, PB, Brazil, 2014 (in Portuguese)
- [20] Gomes Neto, A., e Silva, J.C., de Carvalho, J.N., *et al.*: 'Bandpass frequency selective surface using asymmetrical slot four arms star geometry', *Microw. Opt. Technol. Lett.*, 2016, **58**, (5), pp. 1105–1109